

Energy transfer in turbulence using Lattice Boltzmann Method based on large-eddy simulation

Insaf MEHREZ*, Ramla GHEITH* and Fethi ALOUI**¹

* University of Monastir, National Engineering School of Monastir (ENIM), LESTE Laboratory
Avenue Ibn El Jazzar 5019 Monastir, Tunisia

** Université Polytechnique Hauts-de-France (UPHF), LAMIH, CNRS UMR 8201, INSA Hauts-de-France,
Campus Mont Houy, F-59313 Valenciennes Cedex 9 – France

¹Corresponding author e-mail: Fethi.Aloui@uphf.fr

Abstract

Turbulent flows are characterized by the emergence of simultaneous downscale and upscale energy transfer. The challenge is to control the velocity in two complex geometries. A spectral analysis and a fluctuation velocity were performed on the numerical data obtained from Lattice Boltzmann method (LBM) and large-eddy simulation (LES) of the turbulent flow. In this context, the background of LBM is presented and the construction of Navier-Stokes equations from Boltzmann equation is discussed. The LBM-LES model was developed for solving transition and implanted turbulence modeling. A Fourier transform was chosen to study signals from LBM-LES model and to provide a local analysis of transient turbulent events. The flow in a cavity, as well as the flow around a cylindrical obstacle, were studied with a focus on the evolution of these flows at a high Reynolds number. The simulation results show that the LBM-LES model can produce results in good agreement with other numerical methods and experimental data. It should be noted that this model is easy to apply to complex geometries. The investigated geometries are to be considered a first step that provides, validates, and reliable simulation of the specific properties of the turbulent regime. The behavior of streamlining plots with increasing Reynolds number is exhibited. In the present study, a new method is developed to measure the fluctuating velocity in the turbulent boundary layer. The analyses data were taken from a different position inside the flows, allowing investigation of the turbulent flow. The shear effect on Kolmogorov's -3 power-law scaling of the energy spectrum is discussed.

1. Introduction

This paper is motivated by the need for investigations into the complex interactions of large-scale structures occurring in turbulent flows around obstacles and lid-driven cavities. These flows can be considered as idealizations of such flow situations arising in many engineering applications. The first numerical investigation of the flow in a lid-driven cavity is due to Kawaguti [1] who performed simulations for creeping as well as for nonlinear flows for Reynolds numbers up to $Re=128$, investigating three aspect ratios $\Gamma=0.5, 1, \text{ and } 2$. Only after the more extensive theoretical and numerical study of Bruneau and Saad [2] did the lid-driven cavity become a benchmark problem for Navier–Stokes solvers [3-7] as well as a paradigm for investigating vortex dynamics in closed systems. The second numerical of the flow around the obstacle was performed. Instability and the vortex shedding, caused by the presence of a body in a flow channel, greatly influence the rate of mass transfer between fluid and wall. These phenomena are of great interest in industrial applications because of the possibility of the enhancement of mass transfer. Different studies in the literature have shown that the rate of mass transfer is depending on the control parameters of the flow such as the flow rate, the gap, and the blockage ratio [8-9].

Its main asset is its simple algebraic manipulation, its easy solution procedure and implementation of boundary conditions, together with its ability to deal with complex fluids. This explains why LBM is a very promising and competitive numerical tool in solving heat transfer processes [10-12], turbulent flows [13-14], micro-flows [15-16], nanofluids flow [17-19] porous media [20-22] and multiphase flow [23-26]. However, this apparent simplicity still has some limitations. When trying to simulate turbulent flow, these methods cannot be directly applied. Teixeira [27] presented a lattice Boltzmann method for turbulent flows when the single relaxation time is modified as a variable relaxation time. The large eddy simulation (LES) can efficiently simulate vorticity larger than a prescribed scale. Smagorinsky [28] is applied to simulate flow turbulence, which spread out to be the simplest and most accurate for turbulence flows. Hou et al., [29] demonstrate that the standard Smagorinsky model can be included in the lattice Boltzmann equation for turbulence modeling when the single relaxation time is modified as a variable relaxation time that is directly attached to the distribution function without any calculations of derivatives.

The analysis of sampled signals of turbulent fluid flows through wavelet analysis is now common practice. Such analysis often provides tremendous insight into the flow behavior otherwise difficult to apprehend with more conventional statistical signal analysis methods (example: Fourier transform). The use of wavelet analysis to study signals from LES is not as common, because of the intrinsic high level of non-physical noise introduced by the subgrid models and the reduced resolution both in time and in space. However, depending on the subgrid model and the numerical method, these difficulties may be overcome.

The paper is organized as follows; Section 2 presents the formulation of the lattice Boltzmann Method. Section 3 provides the validation of the proposed method through comparisons with literatures results. Section 4 present the spectral analysis for different position inside the flow. Section 5 concludes the paper.

2. Mathematical formulation

The conventional numerical approach for turbulent flows is the LBM-LES model. However, it is a spatial average over a small volume. Due to the nonlinearity of the Navier Stokes equations models are needed in order to complete the averaged equations, which are termed subgrid-scale models in LES. The incompressible Navier-Stokes equations are numerically solved:

$$\frac{\partial \bar{u}_j}{\partial x_j} = 0 \quad (1)$$

$$\frac{\partial \bar{u}_i}{\partial t} + u_j \frac{\partial \bar{u}_i}{\partial x_j} = -\frac{1}{\rho} \frac{\partial p}{\partial x_i} + \nu \frac{\partial}{\partial x_j} \left(\frac{\partial \bar{u}_i}{\partial x_j} + \frac{\partial \bar{u}_j}{\partial x_i} \right) \quad (2)$$

Lattice Boltzmann method (LBM) is carried out by solving the above governing equations, using large eddy simulation (LES).

2.1. Standard LBM

The lattice Boltzmann model was proposed to solve the axial and radial velocities by (Qian et al., 1992). The equation of the particle velocity distribution function f_k can be written:

$$f_k(\mathbf{r} + \mathbf{e}_k \Delta t, t + \Delta t) = f_k(\mathbf{r}, t) - \frac{\Delta t}{\tau} [f_k(\mathbf{r}, t) - f_k^{eq}(\mathbf{r}, t)] \quad (3)$$

where, f_k is the distribution function denoting the number of particles at lattice node \mathbf{r} and time t , τ is the relaxation time, f_k^{eq} is the equilibrium distribution function and Δt is the time step.

For the D_2D_9 lattice arrangement, τ and f_k^{eq} are given by the following expressions:

$$\tau = \frac{3\nu}{|\mathbf{e}_k|^2} + \frac{\Delta t}{2} \quad (4)$$

$$f_k^{eq}(\mathbf{r}, t) = w_k \rho(\mathbf{r}, t) \left[1 + \frac{3 \mathbf{e}_k \mathbf{U}}{c_s^2} + \frac{9 \mathbf{e}_k \mathbf{U}}{2c_s^4} - \frac{3U^2}{2c_s^2} \right] \quad (5)$$

where ν is the viscosity, U is the velocity vector. The nine velocities \mathbf{e}_k and their corresponding weights w_k in the $D2Q9$ lattice are defined as:

$$\mathbf{e}_0 = (0,0), \mathbf{e}_1 = (\pm 1,0).c, \quad (6)$$

$$\mathbf{e}_{2,4} = (0, \pm 1).c, \mathbf{e}_{5,6,7,8} = (\pm 1, \pm 1).c$$

$$w_0 = \frac{4}{9}, w_{1,2,3,4} = \frac{1}{9}, w_{5,6,7,8} = \frac{1}{36} \quad (7)$$

where $c = \Delta x / \Delta t$; c_s is the speed of sound and Δx is the grid size.

At each node, the macroscopic density ρ and velocity U are calculated from the values of f_k over all directions:

$$\rho(\mathbf{r}, t) = \sum_{k=0}^8 f_k(\mathbf{r}, t) \quad (8)$$

$$u(\mathbf{r}, t) = \frac{1}{\rho} \sum_{k=0}^8 f_k(\mathbf{r}, t) \quad (9)$$

2.2. LBM assembling with LES

LBM-LES is implemented to simulate turbulent flow. To simplify the problem in this study, we assembled the standard Smagorinsky sub-grid scale model [28] into the LBM. By the LES theory, the viscosity is the sum of the molecular and eddy viscosities, ν and ν_t , respectively:

$$\nu_{tot} = \nu + \nu_t \quad (10)$$

ν_t is determined as follows:

$$\nu_t = C_s \Delta * |\bar{S}| \quad (11)$$

Here, C_s represents the Smagorinsky constant, Δ is the filter width, and \bar{S} is the strain rate tensor at the grid-scale. Meanwhile, according to LBM theory, the total viscosity ν_{tot} is calculated as:

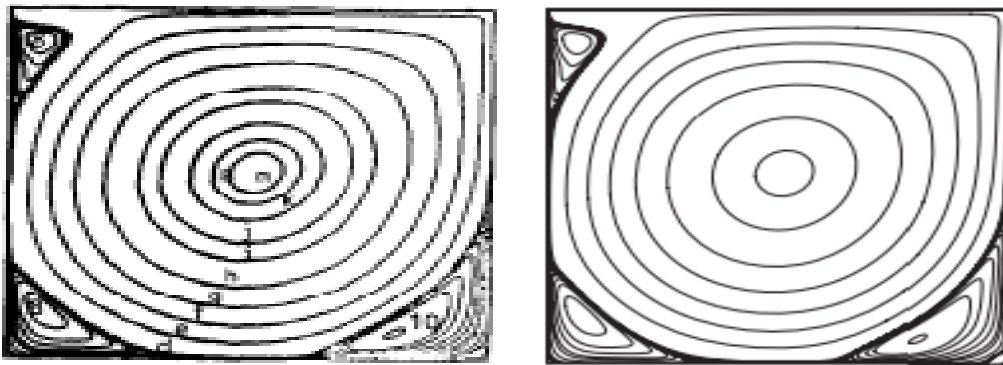
$$\tau_{tot} = 3\nu_{tot} \frac{\Delta t}{\Delta x^2} + \frac{1}{2} \quad (12)$$

where τ_{tot} is the total relaxation time and it is obtained from ν_{tot} , and is used to replace the original relaxation time τ in Eq. (4). As the solution of the lattice Boltzmann (Eq. 3) is the solution to the flow (Eq.1) and (Eq.2), the flow turbulence can be simply and naturally modeled in the standard lattice Boltzmann equation with the total relaxation time which includes the eddy relaxation time from Eq. (10). By using the Chapman-Enskog analysis, it can be showed that the following 2D incompressible turbulent flow can be recovered from the lattice Boltzmann. The present study concentrates on the investigation of flow properties of engineering interest, such as turbulent flow structures in the near wake. The comparison with the other data is carried out, by which the performance of the numerical model can be evaluated.

3. Validations

3.1. Lid drive cavity

The two-dimensional flow in the (x, y) plane can be thought of being implanted in the three-dimensional problem by ejecting the two-dimensional flow field $u = (u, v, 0)$ in z -direction and by letting $Lz \rightarrow \infty$. The numerical calculation of two-dimensional cavity flows requires few resources. The system thus provides a good testbed for numerical codes and for studying two-dimensional flows physics. The square cavity consists of three rigid walls with Bounce-Back scheme and a lid moving with a tangential unit velocity. We are interested in the velocity distribution for a Reynolds number equal to 5000, 7500, and 10000. The corresponding Mach number is $Ma=U/c_s = 0.14$. The simulation used 325×325 uniform meshes. The distance between adjacent nodes was $\delta x = 1$ lattice units (lu) = 0.001m. The time step was set to be $\delta t = 0.001$ s. Following Equation (10), the viscosity of the fluid was $\nu = 3.1 \times 10^{-6}$ m²/s with a relaxation parameter value of 1.9683.



(a)

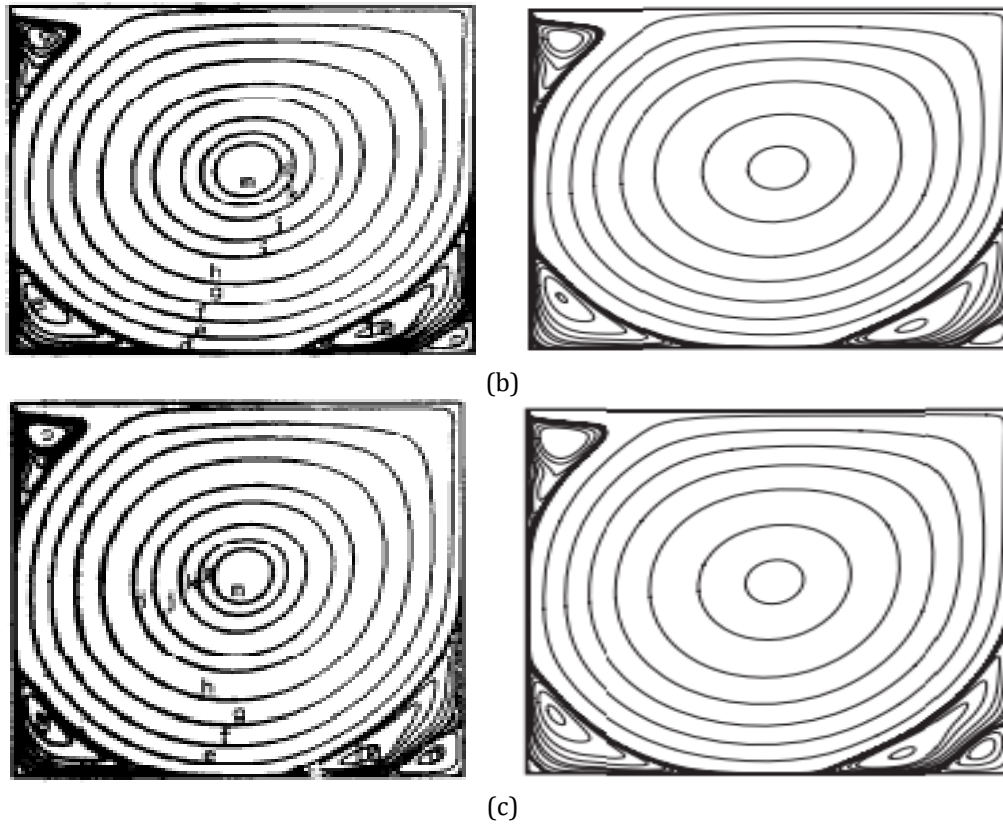


Figure 1: Streamline of Ghia et al., [30] (right) and LBM-LES model (left) for (a) $Re=5000$, (b) 7500 , (c) et $Re=10000$

Typical streamline patterns of the two-dimensional global recirculation vortex driven by the moving wall for $Re = 5 \times 10^3$, 7.5×10^3 and 10^4 are shown in figure 2. The results of LBM-LES model are in good agreement with the results of Ghia et al., [30]. For $Re=5 \times 10^3$, two separated eddies in the bottom corners are signaled by the two separating streamlines. Even a second separated vortex is visible in the bottom right corner. When Reynolds number increase, two more little vortices develop around the secondary vortex at $Re=7.5 \times 10^3$ and $Re=10^4$.

Table 1 show the comparison of the primary vortex (PV) and secondary vortex positions with Erturk results [31]. The abbreviations BR, BL, and TL refer to the cavity's bottom right, bottom left, and top left, respectively. The number after these abbreviations correspond to size of vortex. For all Reynolds number, the relative error is less than 0.55% and 0.89% at the axe-x and the axe-y, respectively. Such a low value was chosen to ensure the accuracy of the LBM-LES model.

Table 1: Comparison of the primary vortex (PV) and secondary vortex positions with Erturk [31]

	Re=5000		Re=7500		Re=10000	
	[31]	LBM-LES	[31]	LBM-LES	[31]	LBM-LES
PV	(0.5146 ;0.5352)	(0.5206 ;0.5325)	(0.5137 ;0.5322)	(0.5137 ;0.5315)	(0.5117 ;0.5303)	(0.5120 ;0.5311)
BR1	(0.8057 ;0.0732)	(0.8095 ;0.0655)	(0.7910 ;0.0654)	(0.7908 ;0.0643)	(0.7754 ;0.0596)	(0.7754 ;0.0588)
BL1	(0.0732 ;0.1367)	(0.0655 ;0.1400)	(0.0645 ;0.1523)	(0.0643;0.1514)	(0.0586 ;0.1621)	(0.0587;0.1632)
TL1	(0.0635 ;0.9092)	(0.0621 ;0.9051)	(0.0664 ;0.9121)	(0.0655 ;0.9112)	(0.0703 ;0.9111)	(0.0703 ;0.9123)
BR2	(0.9785 ;0.0186)	(0.9767 ;0.0164)	(0.9521 ;0.0420)	(0.9512 ;0.0411)	(0.9355 ;0.0674)	(0.9342 ;0.0647)

BL2	(0.0078 ;0.0078)	(0.0074 ;0.0073)	(0.0107 ;0.0117)	(0.0098 ;0.0109)	(0.0166 ;0.0205)	(0.0169;0.0209)
TL2	-----	-----	(0.0010 ;0.0010)	(0.0012 ;0.0015)	(0.0010 ;0.0010)	(0.0012 ;0.0014)
BR3	(0.9990 ;0.0010)	(0.9000 ;0.0011)	(0.9971 ;0.0029)	(0.9965 ;0.0022)	(0.9961 ;0.0039)	(0.9951 ;0.0029)

3.2. Flow around obstacle

The flow around a circular obstacle was investigated as a second case. Obstacles of diameter ranging to $D=10$ lattice units were positioned vertically centered in the first fourth section of the computational domain with sizes $L \times H = 200 \times 50$ lattice units. The rectangular domain refers to the two-dimensional plane (x-y plane) which is perpendicular to the axis of the obstacle. Physical parameters are still available in the lid-driven cavity. For the walls, a no-slip boundary condition was realized. A parabolic velocity inflow profile was applied, and the outlet pressure was fixed. The flow around the obstacles placed inside a channel was simulated for Reynolds numbers $Re = 3900$. The distribution of velocity and vorticity are presented in figure 2. We notice a detachment of the vortices and an appearance of small structures is also clear, at the surface of the cylinder. These results are in closer agreement with Lourenco and Shi results [32]

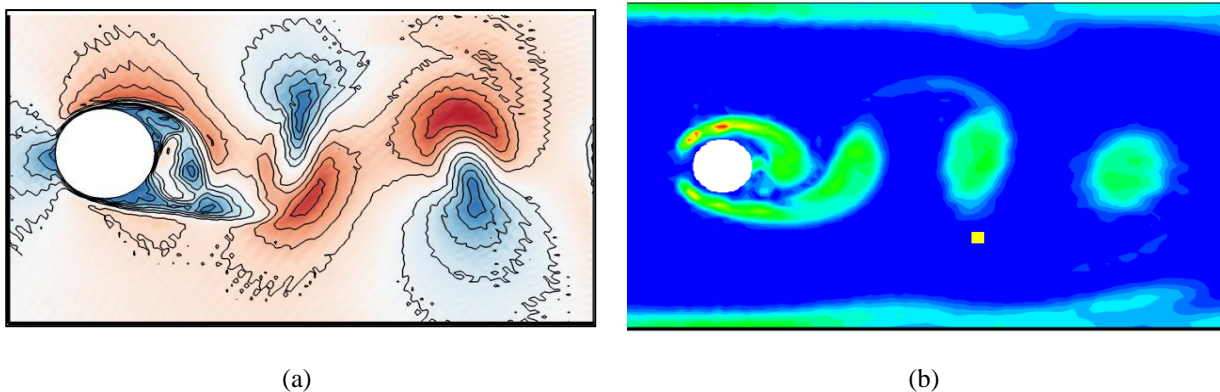


Figure 2: Distribution of a) velocity and b) vorticity for $Re=3900$

In figure 3, a good agreement is obtained at $x = 1.06D$, like at $x = 2.02D$ between our LBM-LES model, [32] and [33]. In particular, a pronounced feature is the V-shape velocity profile at $x/D = 1.06$ in contrast with the U-shape (flat) profile at $x = 2.02D$. The V and U-shape were obtained by using the Smagorinsky model and $k-\epsilon$ model, respectively.

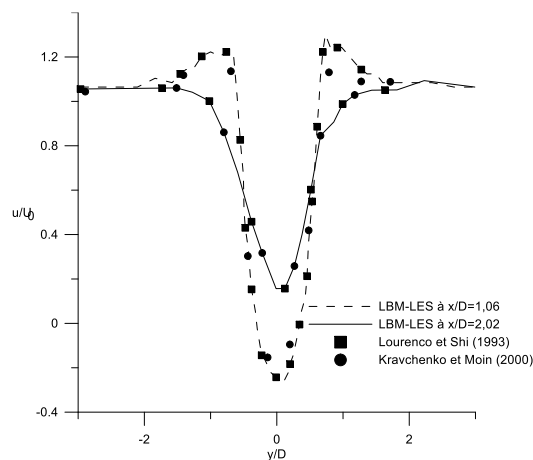


Figure 3 : Comparison of axial velocity between LBM-LES, Lourenco and Shi [32] and Kravchenko and Moin [33] at $x/D=1.06$ and $x/D=2.02$

4. Spectral analysis

For lid-driven cavity, two points have been carefully and purposely elected inside the cavity with a location corresponding to the center and the bottom vortex. The point P1 is located at the center of the cavity with coordinates $P1 = (0.5, 0.5, 0.0)$. The point P2 is located in the BD1 vortex with coordinates $P2 = (0.07, 0.07, 0.0)$

For flow around an obstacle, two points also have been carefully elected inside the rectangular. The P3 is locked at $x/D=1.06$ and the second one is locked at $x/D=2.02$, noted P4.

The time series of the x - y components of the velocity field have been extracted from the LBM-LES databases at the three distinct locations inside the rectangular introduced in the previous section. The groundbreaking work of Kolmogorov [34] highlights the fact that the velocity fluctuations of a turbulent flow can be characterized and analyzed based upon the behaviors of the scales of the spatial increment of the Eulerian velocity of the Lagrangian velocity. A pre-analysis of the simulated system consists of the Fourier transform computation applied to the velocity signal at the points (P1, P2) and (P3, P4) of maximum mean turbulence production within the cavity. The Fourier transformation can be written as:

$$S(\nu) = \int s(t)e^{-2i\pi\nu t} dt \quad (13)$$

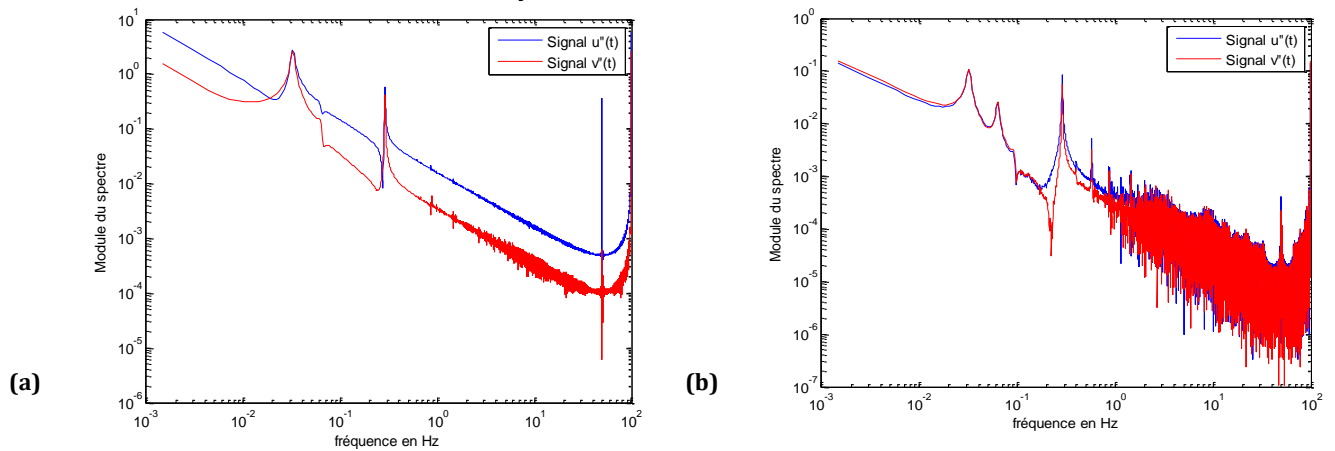


Fig. 4: Fourier transforms of the time histories of the LBM-LES velocity signals maximum mean turbulence production within the cavity at a) the point P1 and b) the point P2

The results of the spectral analysis for the intensity in a Log-Log scale are shown in Figure 4 where a $-5/3$ slope is observed for the velocity signals. These results, which are characteristics of the developed turbulence region of the cavity flow are in good agreement with those predicted by the statistical theory of the turbulence [34]. Slopes were conventionally estimated using a linear regression method. It is worth noting that these spectra lack smoothness at high frequencies due to the limited size of our databases of turbulent flow samples.

The above results for the turbulent region of the flow, for different positions, provide structures possessing a clear fractal signature. The P1 is characterized by a small frequency corresponding to the gravity force and the P2 corresponds to very large depressions associated with the turbulent bursts occurring when a pair of counter-rotating vortices is produced. At this position, we note the absence of the small frequencies.

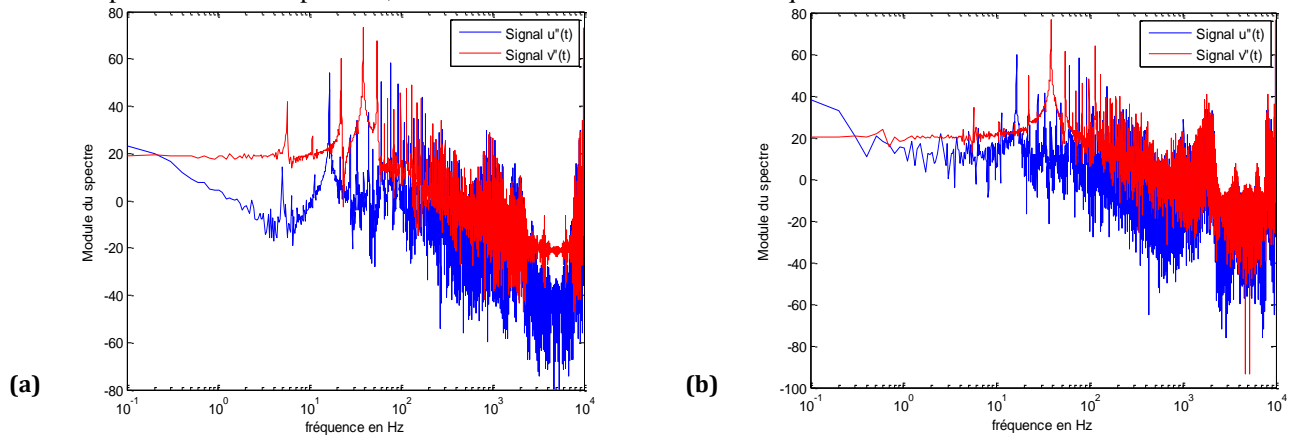


Fig. 5 Fourier transforms of the time histories of the LBM-LES velocity signals maximum mean turbulence production within the flow around obstacle at a) the point P3 and b) the point P4

The energy spectrum obtained at different positions in a statistically stationary flow is shown in figure 5. A dual cascade clearly develops. In the stationary regime, the spectrum displays at P3 a scaling compatible with $E(k) \sim k^{-5/3}$. For the spectrum at P4, more frequencies are apparent and present a $E(k) \sim k^{-3}$ scale law. The low exciting frequency is about 100 Hz (2s period). This characteristic frequency is shown with the analytical value calculated for Strouhal number $St=0.187$, $U_0=1.5$ m/s, $H=1$ cm, and $d=3.33$ mm.

5. Conclusions

For different cases, we were able to show that our implementation of the LBM-LES yields reliable results. By using this new source formulations, relatively simple and easy to implement, have been successfully investigated. The fluctuation of the instantaneous velocity fields inside the cavity and around obstacles are then used to investigate the complex vortical structures which characterize this flow. The LBM-LES is an alternative approach to the Navier–Stokes equation (NSE) to solve fluid flow problems. This method is capable of modeling applications such as turbulent flow. Solution of the lattice Boltzmann equation (LBE) uses a simple stream and collide computational procedure. Although the most popular formulation of the LBE is the Boltzmann equation with the so-called Bhatnagar Gross Krook (BGK) approximation based on the use of a single relaxation time (SRT). The simple and traditional spectral (Fourier) analysis presented provides interesting initial results. However, such spectral analysis is known to provide limited insight.

Acknowledgments

This research was supported by the laboratories LESTE of ENIM (university of Monastir, Tunisia) and LAMIH (UMR CNRS 8201) of the Université Polytechnique Hauts-de-France (Valenciennes, France). These supports are gratefully acknowledged.

References

- [1] Kawaguti, M., 1961. Numerical solution of the Navier–Stokes equations for the flow in a two-dimensional cavity. *J. Phys. Soc.Jap.*, 16:2307–2315.
- [2] Bruneau, C.H., Saad, M., 1977. The 2d lid-driven cavity problem revisited. *Comp. Fluids*, 35:326–348, 2006
- [3] Schreiber, R., Keller, H.B., 1983. Driven cavity flows by efficient numerical techniques. *J. Comput. Phys.*, 49:310–333, 1983
- [4] Ghia, K., Ghia, N., Shin, C.T. 1982. High-Re solutions for incompressible flow using the Navier-Stokes equations and a multigrid method. *J. Comput. Phys.*, 48: 387–411, 1982.
- [6] Botella, O., Peyret, R., 1998. Benchmark spectral results on the lid-driven cavity flow. *Comp. Fluids*, 27:421–433.
- [7] Albensoeder, S., Kuhlmann, H.C., 2005. Accurate three-dimensional lid-driven cavity flow. *J. Comput. Phys.*, 206:536–558.
- [8] Zheng, G. S., and Worek, W. M., 1996, “Methods of Heat and Mass Transfer Enhancement in Film Evaporation,” *Int. J. Heat Mass Transfer*, 39(1), pp. 97–108.
- [9] Berger, F. P., Hau, K.-F., and Hau, F.-L., 1979, “Local Mass/Heat Transfer Distribution on Surfaces Roughened With Small Square Ribs,” *Int. J. Heat Mass Transfer*, 22(12), pp. 1645–1656.
- [10] S. C. Mishra, and A. Lankadasu, Application of the lattice Boltzmann method for solving the energy equation of a 2-D transient conduction–radiation problem, *Numer. Heat Transfer A*, vol. 47, pp. 935-954, 2005.
- [11] F. Massailoi, R. Benzi, and S. Succi, Exponential Tails in Two-Dimensional Rayleigh–Bénard Convection, *Europhysics Letters*, vol. 212, pp. 303-310, 1993.
- [12] M. El Abdallaoui, M. Hasnaoui, and A. Amahmid, Lattice-Boltzmann modeling of natural convection between square outer cylinder and an inner isoscles triangular heating body, *Numer. Heat Transfer A*, vol. 66, pp. 1076-1096, 2014.
- [13] C. M. Teixeira, Incorporating Turbulence Models into the Lattice-Boltzmann Method, *Int. J. Modern Physics C*, vol. 9, No. 8, pp. 1159-1175, 1998.
- [14] H. Yu, S. S. Girimaji, and L. S. Luo, DNS and LES of decaying isotropic turbulence with and without frame rotation using lattice Boltzmann method, *J. of Computational Physics*, vol. 209, pp. 599–616, 2005.
- [15] X. Nie, G. D. Doolen, and S. Chen, Lattice Boltzmann simulation of fluid flows in MEMS, *J. of Statistical Physics*. vol. 107, pp. 279-289, 2002.

- [16] C. Y. Lim, C. Shu, X. D. Niu, and Y. T. Chew, A lattice Boltzmann BGK model for simulation of micro flows, *Physics of fluids*, vol. 14, pp. 2299-2308, 2002.
- [17] A. H. Saberi, and M. Kalteh, Numerical investigation of nanofluid flow and conjugate heat transfer in a micro-heat-exchanger using the lattice Boltzmann method, *Numer. Heat Transfer A*, vol. 70, pp. 1390-1401, 2016.
- [18] S. Savithiri, A. Pattamatta, and S. K. Das, A single-component nonhomogeneous lattice Boltzmann model for natural convection in Al₂O₃/water nanofluid, *Numer. Heat Transfer A*, vol. 68, pp. 1106-1124, 2015.
- [19] W. N. Zhou, and Y. Y. Yan, Numerical investigation of the effects of a magnetic field on nanofluid flow and heat transfer by the lattice Boltzmann method, *Numer. Heat Transfer A*, vol. 68, pp. 1-16, 2015.
- [20] L. Chen, W. Fang, Q. Kang, J. De'Haven Hyman, H. S. Viswanathan, and W.-Q. Tao, Generalized lattice Boltzmann model for flow through tight porous media with Klinkenberg's effect, *Phys. Rev. E*, vol. 91, 033004, 2015.
- [21] Z. Guo and T. S. Zhao, Lattice Boltzmann model for incompressible flows through porous media, *Phys. Rev. E*, vol. 66, 036304, 2002.
- [22] S. C. Mishra, S. Panigrahy, and V. J. Ghatage, Analysis of combined mode heat transfer in a porous medium using the lattice Boltzmann method, *Numer. Heat Transfer A*, vol. 69, pp. 1092-1105, 2016.
- [23] Y. Hu, D. C. Li, S. Shu, and X. D. Niu, Immersed boundary-lattice Boltzmann simulation of natural convection in a square enclosure with a cylinder covered by porous layer, *Int. J. of Heat and Mass transfer*, vol. 92, pp. 1166-1170, 2016.
- [24] S. Chen and G. Doolen, Lattice Boltzmann for fluid flows, *Annual Review of Fluid Mechanics*. vol. 30: pp. 329-364, 1998.
- [25] X. Chen and H. Chen, Lattice Boltzmann model for simulating flows with multiple phases and components, *Phys. Rev. E*, vol. 47, 1815, 1993.
- [26] X. Y. He, S. Y. Chen, and R. Zhang, A Lattice Boltzmann Scheme for Incompressible Multiphase Flow and Its Application in Simulation of Rayleigh-Taylor Instability, *J. of Computational Physics*. vol. 152, pp. 642-663, 1999.
- [27] Teixeira, C. M., 1998. Incorporating Turbulence Models into the Lattice-Boltzmann Method, *Int. J. Modern Physics C*, vol. 9, No. 8, pp. 1159-1175.
- [28] Smagorinsky J., 1963. General circulation experiments with the primitive equations. *Mon. Weather Rev*, Vol. 91, pp. 99-164.
- [29] Hou S., Sterling J., Chen S., Doolen G.D., 1996. A lattice Boltzmann subgrid model for high Reynolds number flows. *Fields Inst. Commun*, Vol. 6, pp. 151-166
- [30] Kolmogorov, AN., 1941. The local structure of turbulence in incompressible viscous fluid for very large Reynolds numbers. *CR AcadSci USSR*, 299-303.